Fermilab

Project Notes
DRAFT: June 26, 2013

Collimation with hollow electron beams

Giulio Stancari and Alexander Valishev
Fermi National Accelerator Laboratory, P.O. Box 500, Batavia, IL 60510, U.S.A.

Abstract

Magnetically confined hollow electron beams for controlled halo removal in high-energy colliders such as the Tevatron or the LHC may extend traditional collimation systems beyond the intensity limits imposed by tolerable material damage and impedance. They may also improve collimation performance by suppressing loss spikes due to beam jitter and by increasing capture efficiency. The goal of this project is to test whether the hollow-beam collimation concept is viable and to assess its limitations.

Contents

1 Introduction

In high-energy colliders, stored beam energy can be large. At the Tevatron, at the beginning of a collider store, the total energy of the proton beam is $(3 \times 10^{11}$ particles/bunch$) \cdot (36$ bunches$) \cdot (1$ TeV/particle$) \cdot (1.6 \times 10^{-19}$ J/eV$) = 1.7$ MJ. The LHC beam at full intensity is expected to have an energy of almost 400 MJ.

Uncontrolled losses of even a small fraction of the circulating beam can damage sensitive components, quench superconducting magnets, or produce intolerable experimental backgrounds.

Beam-beam collisions, intrabeam scattering, beam-gas scattering, rf noise, ground motion, resonances, etc. contribute to the formation of the beam halo.

The goals of collimation are to protect the apparatus by eliminating the halo and by directing losses to well-controlled regions. Conventional schemes involve (primary) collimators and absorbers (or secondary collimators). In the Tevatron, the collimators are 5-mm tungsten plates positioned about 5 standard deviations away from the center of the beam core. The absorbers are 1.5-m steel jaws at 6σ [1]. In the LHC, the collimators are 0.6-m carbon jaws at 6σ, whereas the 1-m carbon/copper absorbers are positioned at 7σ [2].

The performance or efficiency of a collimation system is measured by the fraction of the total losses that are intercepted by the absorbers. It depends on the phase advance between the collimators and the absorbers. The collimation system must ensure a tolerable dose level both in the case of normal operations and of unintentional beam aborts.

Project supported by U.S. LARP in collaboration with the LHC Collimation Working Group. Letters of support from CERN Directorate and recommendations form Fermilab AAC.

2 Project history

Summer 2009: hollow gun design (Kuznetsov, Vorobiev); TEL2 BPM software upgrade (Romanov).

August 2009: 0.6-in hollow gun manufactured by Hi-Tech Mfg., delivered Aug 27.

Fall/winter 2009/2010: hollow beam dynamics in test stand (Valishev, Stancari); TEL2 BPM calibrations (Valishev, Stancari).

August 2010: hollow gun installed in TEL2 (Kuznetsov, Sylejmani, Stancari); complete system test (Saewert, Simmons, Crisp, Fellenz, Kuznetsov, Zhang, Stancari); verified abort-gap clearing (Zhang).

October 2010: first Tevatron experiments (Valishev, Stancari).

February 2011: I. Morozov joins group for 1 year on simulations. A. Didenko joins for 6 months on design of 1-inch cathode.

March 2011: new scintillator paddles installed near F49 pbar absorber, gated loss monitors T:LF49T{1,2,3} logged at 15 Hz starting Apr 14.

June 2011: LHC Collimation Review, https://indico.cern.ch/event/139719

August 2011 – July 2013: V. Previtali joins group as Toohig fellow. Simulations of halo diffusion and beam scraping in the SPS and in the LHC with Lifetrac and Sixtrack.

September 2011: end of Tevatron run.

October 2011: 1-in gun (HG1) installed in test stand.

January–February 2012: first characterization of 1-in hollow gun.

June–August 2012: Siqi Li (Lee Teng summer intern from the University of Chicago) joins to work on 1-in gun characterization and improvements.

14 August 2012: the 1-in hollow gun (now renamed HG1b) was modified to reduce the quadrupole pattern in the current density profile. Added stainless-steel cylinder to shield cathode-anode gap from support legs.

October–December 2012: first characterization of modified 1-in hollow gun.

November 2012: internal review of hollow electron beam collimation at CERN, https://indico.cern.ch/event/213752.

January 2013: LIU-SPS beam scraping system review, https://indico.cern.ch/event/221617.

January–February 2013: visit of Korean students, Boo-Seung Yang, Jin-Seok Kim, Young-Hyun Cho, from Prof. Hae June Lee's group at Pusan National University, to work on 2D simulations of hollow electron beam profile evolution.

February–May 2013: Vince Moens, undergraduate student from *École Polytechnique Fédérale de Lausanne*, Switzerland, supervised by Leonid Rivkin (EPFL) and Stefano Redaelli (CERN), visits Fermilab to work on the application of hollow electron beam collimation to the LHC.

February–May 2013: detailed study of modified 1-in hollow gun. Significantly improved electron beam transport.

10 June 2013: review of proposed LARP contributions to the LHC luminosity upgrade, https://indico.fnal.gov/event/6836.

3 Resources

- Electron-lens Redmine wiki.
- Electronic logbook (accessible from the Fermilab site).
- AFS disk space: /afs/fnal.gov/files/data/apc/hebc.

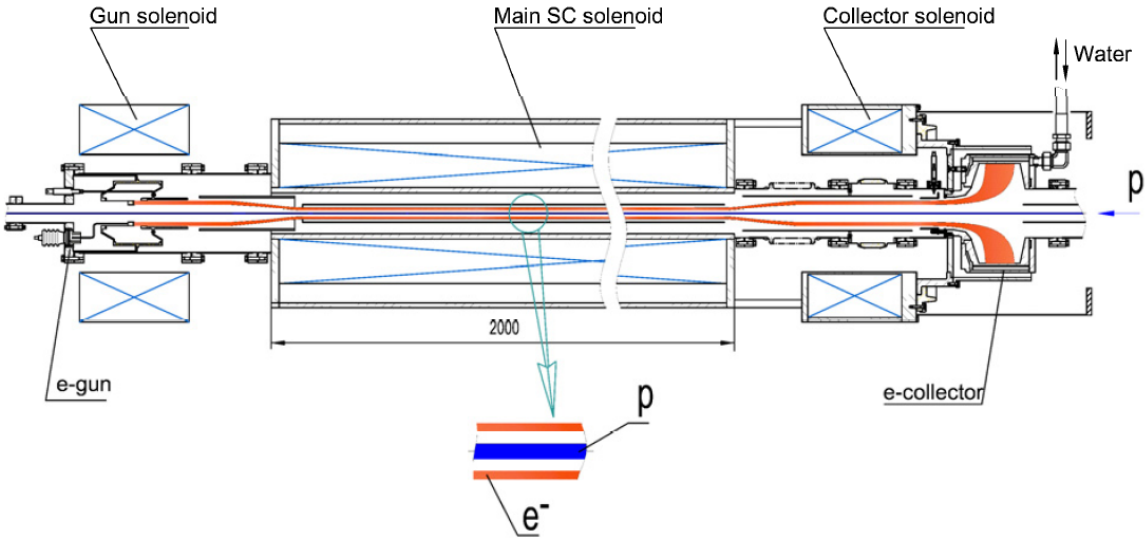

Figure 1: Concept of hollow electron beam collimator. *(ADD PLOT OF CURRENT DENSITY AND KICKS)*

4 Concept

The hollow electron beam collimator (HEBC) is a magnetically confined, possibly pulsed electron beam with a hollow current-density profile overlapping with the proton or ion beam of interest (Figure 1). The core passes through the center of the electron distribution and is unperturbed. The halo experiences nonlinear transverse kicks and it is driven towards the absorbers [3, 4].

The electron gun is immersed in a conventional solenoid and provides a few amperes of current at 10 keV. The overlap region is contained within the cryostat of a superconducting solenoid providing an axial field of up to 6 T. The electron beam is then driven towards a water-cooled collector inside a separate conventional solenoid.

The sizes r_{main} of the hollow beam in the interaction region (hole, edges, etc.) are determined by the corresponding sizes at the gun r_{gun} and by the 'compression ratio' of gun to main solenoid strength:

$$r_{\mathrm{main}} = r_{\mathrm{gun}} \sqrt{\frac{B_{\mathrm{gun}}}{B_{\mathrm{main}}}} \tag{1}$$

Besides the maximum technologically achievable fields in the gun and main solenoids, electron transport efficiency and instability thresholds can influence the range of available beam sizes in the overlap region.

The main appeal of this technique is that the electron beam can be placed close to an intense beam core without any material damage. At present, there is no viable solution for beam scraping in the LHC at full intensity: no material can be brought closer than 5σ.

The maximum kick experienced by protons traversing a hollow electron beam of current I and outer

radius $r_{\max}$ in an interaction region of length L is given by the following expression:

$$\theta^h_{\max} = \frac{2IL(1 \pm \beta_e \beta_p)}{r_{\max} \beta_e \beta_p c^2 (B\rho)_p} \left(\frac{1}{4\pi\varepsilon_0} \right), \tag{2}$$

where $\beta_e c$ is the electron velocity, $\beta_p c$ the proton velocity, and $(B\rho)_p$ is the magnetic rigidity of the proton beam. The $+$ sign applies when the magnetic force is directed like the electrostatic attraction ($\mathbf{v}_e \cdot \mathbf{v}_p < 0$), whereas the $-$ sign applies when $\mathbf{v}_e \cdot \mathbf{v}_p > 0$. For example, in a configuration similar to a Tevatron electron lens ($I = 2.5$ A, $L = 2$ m, $\beta_e = 0.19$, $r_{\max} = 3.5$ mm), the corresponding kicks are $\theta_{\max} = 2.4$ μrad for 150-GeV protons and 0.36 μrad at 980 GeV.

In the overlap region, it is preferable to have large amplitude functions β_x and β_y, so that the corresponding position displacements at the collimators or absorbers (proportional to $\sqrt{\beta_{x,y}}$) are amplified. The symmetry of the system and the $\mathbf{E} \times \mathbf{B}$ twist of the electrons around the axis as they propagate would require $\beta_x = \beta_y$. If this is not the case, separate horizontal and vertical scrapes can be performed, either by scanning twice with one HEBC or by using 2 separate HEBCs.

In each plane, the rms kicks of a conventional collimator due to multiple Coulomb scattering are

$$\theta^c_{\text{rms}} = \frac{(13.6 \text{ MeV}) \cdot z}{\beta c p} \sqrt{\frac{x}{X_0}} \left[1 + 0.038 \cdot \ln\left(\frac{x}{X_0} \right) \right], \tag{3}$$

where z, βc and p are the projectile's charge state, velocity and momentum, and x and X_0 are the thickness and radiation length of the collimator ($X_0 = 3.5$ mm for tungsten). For the Tevatron collimators, the rms kicks are 110 μrad at 150 GeV and 17 μrad at 980 GeV. At 7 TeV, the LHC collimators impart an rms kick of 4.5 μrad. Very large electron currents would be necessary for the HEBC to provide the same kicks as a conventional collimator and clean halo particles in a few revolutions.

One important difference between the HEBC and conventional schemes is that the hollow-beam kicks are not random in space or time. The electric field is determined by the electrons' current distribution, and the electron beam can be continuous or pulsed once every given number of turns with rise times below 100 ns. Resonant excitation tuned to a strong lattice resonance is possible. This technique is very effective, as demonstrated by calculations (see below) and by abort-gap clearing with electron lenses tuned to the 3rd and 7th order resonances in the Tevatron [7].

From these considerations, the HEBC emerges as a 'soft scraper' to complement and improve a conventional collimation system. The electron beam has no hard edges, losses are gradual, and loss spikes due to beam jitter are reduced (*ADD FIGURE OF TOTAL AND ABORT-GAP LOSSES DURING STORE*. Flying wires intercepting the beam every hour does not affect the overall picture). The impact parameter on the primary collimators is increased, and they may be retracted to reduce impedance, if protection of the apparatus is not compromised.

There are other advantages. In the case of ion-beam cleaning, there is no nuclear breakup. Collimator positions are controlled by magnetic correctors, and not by mechanical means. More importantly, both extensive theoretical modeling and technical experience are available on the interaction of low-energy electrons with high-energy protons from the fields of electron cooling and Tevatron electron lenses [5, 6]. Figure 2 shows a photograph of TEL2, the second Tevatron electron lens, together with its typical parameters.

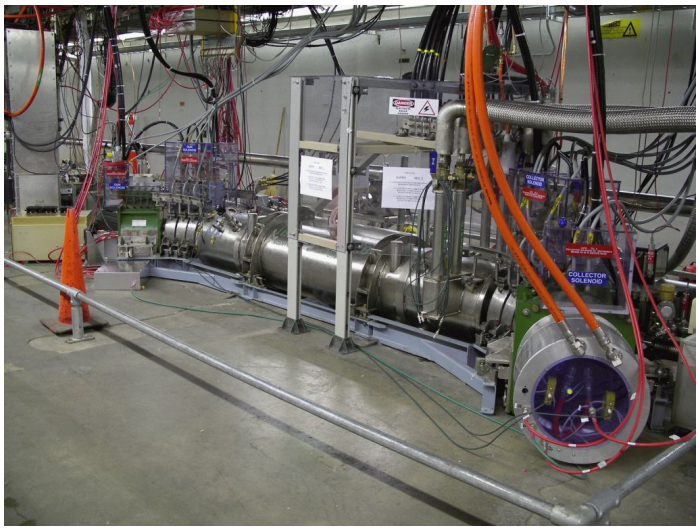

Typical TEL2 parameters	
Peak energy	10 kV
Peak current	3 A
Max gun field B_g	0.3 T
Max main field B_m	6.5 T
Length L	2 m
Rep. period	21 μs
Rise time	$<$200 ns

Figure 2: Photograph of the second Tevatron electron lens and typical parameters.

The stability of the proton-electron system and the impedance of the HEBC need to be investigated in detail. It is known that stability is not an issue for Gaussian or flat beams in a Tevatron electron lens if the confining field is of the order of 2 T or higher. In this case, calculation exist of the treshold for the onset of transverse-mode coupling instabilities [8]. For the HEBC, the situation should be more favorable, as in the ideal case the proton beam experiences no field.

The magnetically confined hollow electron beam itself is not stable under the effect of space charge. Small asymmetries in the initial distribution or in the external field configuration can generate $\mathbf{E}\times\mathbf{B}$ drifts of the centers of gyration that are not cylindrically symmetric. This may lead to profiles that are distorted and which vary over the interaction region, producing undesired fields at the center. Possible correction schemes include azimuthally segmented control electrodes near the cathode or exploitation of the natural $\mathbf{E}\times\mathbf{B}$ drift. These issues are discussed in more detail below.

Alignment of the beams is critical. HEBC design should include magnetic correctors and beam position monitors. Field line ripple can be controlled to within 0.1 mm. This size should be small compared to the transverse size of the beams.

An HEBC requires a superconducting magnet for the main solenoid and, therefore, liquid-helium cryogenics. Its total cost is of the order of 5 M$ (2 M$ for material and supplies, 3 M$ for labor).

5 Modeling and simulations

Simulations are used to calculate the effect of the HEBC on the proton beam and to estimate its effectiveness.

5.1 Kick maps

Analytical models of the electron current distribution are used at first for simplicity, such as

$$j(r,\theta,t) = \tag{4}$$

From the measurements of the actual density profiles (described below), a 2D map of the fields can be extracted using a Poisson solver.

Evolution of 2D profiles (diocotron instability) calculated by M. Chung with plasma code based on xpdp2.

As a last stage, a full 3D simulation of the electron beam through the system is being set up using the Warp code [**?**]. The purpose is to take into account such effects as longitudinal profile evolution or TEL2 bends. If the latter turn out to be irrelevant, the electron lens configuration can be adopted instead of the fully symmetrical one depicted in Figure 1.

5.2 Tracking codes

The field maps are then used by tracking codes to follow core or halo particles as they propagate in the machine lattice, with different levels of refinement: apertures, nonlinearities, beam-beam effects, and so on.

Rough estimate of single-turn amplitude increase near resonant line: $dA = 4\pi A dQ$?

Shiltsev (FERMILAB-CONF-07-69): 1D simulation of position vs turn number in LHC, modulating e-current in phase with tune. Time needed to reach 10-σ amplitude vs lens detuning and vs lens current. Modulation of elens current not critical because of natural beam tune spread: $\Delta Q(\text{halo}) \sim 0.001$, acceptance of modulation technique ~ 0.002.

Drozhdin/Shiltsev (beams-doc-3107): 3D simulation in Tev, 3000 particles, including separators, rf, sextupole correctors and collimators, but kicks are too large. Losses vs elens modulation. Elens is nonlinear; lattice nonlinearities are not taken into account?

Drozhdin, with STRUCT for Tev. Kicks, apertures. Pulsed lens. 0.3 μrad too small, 3 μrad noticeable (80% halo lost in ... turns) as primary collimator.

Valishev, with Lifetrac for Tev. Simplified aperture. No pulsing. Includes nonlinearities and beam-beam. 0.3 μrad very small.

Smith, for LHC with first_impact and SixTrack (PAC09, SLAC-PUB-13745). Collimators at 6σ, 0, 90, 135 deg wrt horizontal. Two Gaussians: core (σ), halo (10σ) overpopulated to show effect.

- 20 A DC at 3σ, 1500 turns without collimators, ¡1000 with collimators. Comparisons of different scenarios: no elens, elens, elens+collimators/absorbers retracted (1, 2, 3σ). Within 1000 turns, halo reduction with elens + retracted collimators (even 3σ!) is the same as conventional system. No apparent advantage of conventional+elens
- large increase in impact parameter.

Switched to BMAD (why?).

To do:

- nonstraight B-field lines
- realistic current profiles
- asymmetric profiles (nonzero E-field in core)
- performance vs lattice parameters

Guest scientist (I. Morozov) to join project in January 2011 for 1 year.

5.3 Diffusion model of collimation

Asymptotic lifetime proportional to admittance/diffusion. Equilibrium rms proportional to aperture.

Effects of changes in admittance or diffusion rate on losses as a function of time.

6 Hollow electron gun design and performance

6.1 Design considerations

A high-perveance gun with negligible central field is necessary to test hollow-beam collimation. Several approaches exist for the design of hollow guns, such as magnetron injection guns []. An axially symmetric hollow electron gun was designed for cooling [**?**].

The present design is based upon the guns already employed in the TELs. A convex tungsten dispenser cathode with BaO–CaO–Al_2O_3 impregnant is used to obtain high perveance [**?**, **?**]. The cathode has an outer diameter of 15.24 mm (0.6 in) and a radius of curvature of .... In this design, a 9 mm-diameter hole is simply bored through the cathode. The expected profile in the space-charge-limited regime was calculated by L. Vorobiev using the Super/UltraSAM code (Figure **??**). The calculated current density distribution vanishes between $0 < r < 4.5$ mm, then rises sharply and gradually goes back to zero at $r = 7.62$ mm (*CALCULATIONS WITH WARP?*)

Axially symmetric configuration.

6.2 The 0.6-in hollow electron gun

15-mm (0.6-in) diameter cathode for TEL2. Same electrode configuration as SEFT gun. Manufactured by Hi-Tech Mfg. in Schiller Park, Illinois using a spherical cathode from Heat Wave. Delivered Aug 27, 2010 and installed in test bench for characterization. Installed in TEL2 Aug 2, 2011.

Performance vs. temperature and voltage.

0.6-in profiles.

Stability of hollow beam. Scaling law of profile evolution.

Profile reproducibility vs. time.

Profile vs. temperature.

Time microstructure of pulse: convex cathode? longitudinal space charge? ions?

6.3 The 1-in hollow electron gun

25-mm (1-in) cathode will yield higher currents; fields and apertures of TEL2 to be verified. Modifications.

Yield vs. temperature and voltage.

Profile measurements.

6.4 Electron lens test stand

Test bench apparatus and techniques.

7 Tevatron experiments

Current collimation scheme. Primary collimators: 5-mm W, L-shaped? at 5σ at E0 (prot.) and F49 (pbar), ... Secondary: 1.5-m L-shaped steel jaws at F17 (prot.) and D17 (pbar). Backgrounds at CDF and D0 mostly generated in inner triplets (large beta). D0 forward Roman pots at 8σ, CDF at 10σ. How are losses measured? $\rightarrow$ Figure with device names.

BPM calibration.

What we plan to measure as a function of HEBC parameters (position, angle, intensity), for individual bunches:

- removal rates;
- core lifetimes;
- losses at collimators and detectors (collimator losses gated by train starting April 14, 2011);
- improvement of spikes due to beam shaking (~ 50 μm, low-beta quads vibrate at a few Hz because of CHL) hitting hard collimators when too close ($< 5\sigma$?);
- effect on diffusion rates.

Luminosity lifetime as indicator of core lifetime. Expected effect of intensity lifetime on luminosity lifetime.

Best to measure at 980 GeV, even though kicks are smaller. At 150 GeV: little time during operations; unstable conditions (growing emittances, orbit drifts); collimators are not normally used. But beam width approximately equal to 980 (larger emittance, lower beta).

Choosing antiprotons: lower emittances and intensities, larger fields, more stable. TEL2 closer to pbar collimator.

Bunch intensities (10^9)	C:FBI{P,A}NG[]
SynchLite beam sizes (mm)	T:SL{P,A}S{H,V}[]
SynchLite beam emittances (μm)	T:SL{P,A}E{X,Y}[]
SBD bunch lengths (ns)	T:SBD{P,A}WS[]
SBD momentum spread (10^{-4})	T:SBD{P,A}WS[]
1.7-GHz Schottky tunes	T:
Tune settings	
Chromaticity settings	
Luminosities	
D0 losses	
CDF losses	
Collimator positions	
Collimator losses, total	
Collimator losses, gated (after Apr 14, 2011)	
TEL2	
solenoids	T:L2S{G,M,C}
correctors	T:L2C{1,2,3,4,5,6}
modulator voltage	T:L2MCV1
collector current	T:L2COLI
Java BPMs	T:{G,C}{P,A,E}{X,Y}

Table 1: ACNET devices. Modulator voltage (T:L2MCV1) and Java BPM positions (T:TL2{G,C}{P,A,E}{X,Y}) started to be logged on Oct 19, 2010.

7.1 Studies cheat-sheet

Tevatron parameters:

f_{RF}	53 104 693 Hz
h	1113
f_{rev}	47 713.111 Hz
T_{rev}	20 958 600 ps
$T_{\mathrm{rev}}/3$	6 986 200 ps
bucket	18 830.728 ps
bunch spacing	395 445.28 ps
η	2.89×10^{-3}

Lattice functions at TEL2 and SyncLight (measured 20 Aug 2010):

	β_x	β_y	D_x	D_y	Q_x	Q_y
TEL2	67.8	153.5	1.25	-1.01	3.175	3.220
p SyncLite	52.7	114.6	1.67	-0.576		
$\bar{p}$ SyncLite	37.6	109.3	1.25	-0.603		

$$\varepsilon = \frac{1}{\beta_{\mathrm{SL}}}\left[\sigma_{\mathrm{SL}}^2 - (D_{\mathrm{SL}}\cdot\delta)^2\right]$$

$$\sigma_{\mathrm{TEL}}^2 = \frac{\beta_{\mathrm{TEL}}}{\beta_{\mathrm{SL}}}\left[\sigma_{\mathrm{SL}}^2 - (D_{\mathrm{SL}}\cdot\delta)^2\right] + (D_{\mathrm{TEL}}\cdot\delta)^2$$

Beam sizes at TEL2 vs. beam sizes at SyncLite.

Choice of main field:

$$B_m = B_g\left(\frac{r_g}{r_m}\right)^2$$

Colliding bunches at A0/D0 and CDF:

	A1	A13	A25
A0, D0	P25	P1	P13
CDF	P13	P25	P1

Delays for protons and antiprotons (check on `tel2scope.fnal.gov`):

trigger mode `T:L2TM`	1	2	4
$\bar{p}$, `T:L2DLY1` $= 627$	A1–A12	A13–A24	A25–A36
p, `T:L2DLY1` $= 631???$	P25–P36	P1–P12	P13–P25

The TEL2 BPM delay should be set to `T:L2DLY0` $= 685$ to be synchronized with protons, antiprotons and electrons (`T:L2TM` $= 2$, slot 15).

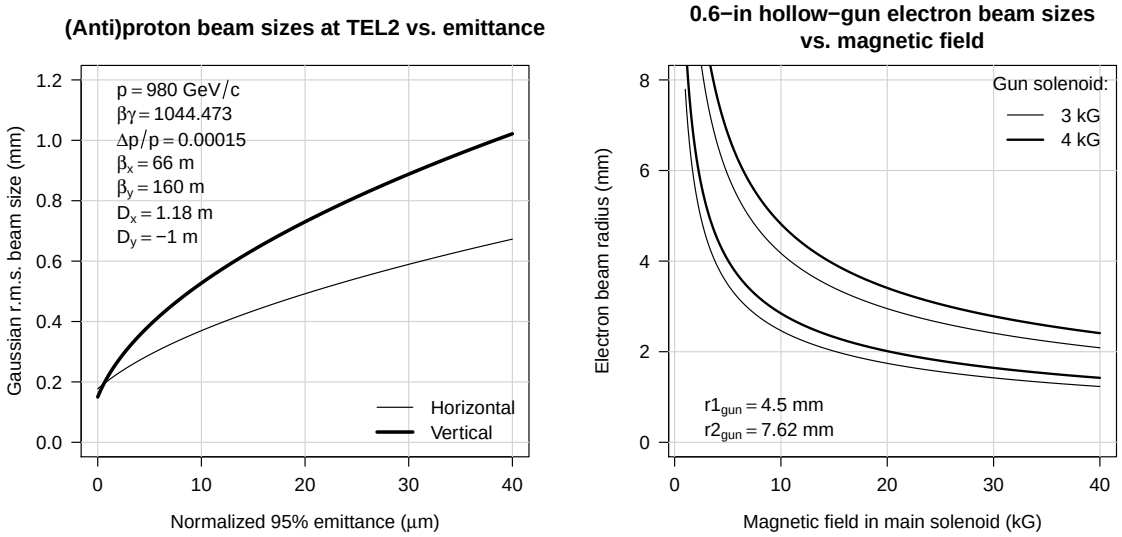

NAME	s	bx	by	Dx	Dy	Qx	Qy
hCF171LD	195.0138	87.4310000	31.3329000	6.7679300	0.19111700	0.63293	0.58832
hCF171LD	196.6902	82.1504000	33.8057000	6.5526800	0.20035400	0.63586	0.59797
hCF172UR	196.8648	81.6138000	34.0793000	6.5302600	0.20131600	0.63618	0.59893
hCF172UR	198.5412	76.5924000	36.8581000	6.3150100	0.21055300	0.63930	0.60778
hCF173LD	205.3135	58.6974200	50.9055000	5.4454500	0.24786800	0.65410	0.63691
hCF173LD	205.5611	58.1156500	51.5049000	5.4136500	0.24923300	0.65471	0.63780
hCF48RD	966.5219	92.5302000	29.2385400	0.7572860	-0.26225200	3.08693	2.95705
hCF48RD	968.1983	93.9754000	29.0195500	0.7561830	-0.28596100	3.08965	2.96678
cTEL	968.8793	94.5829000	28.9889900	0.7557180	-0.29563400	3.09074	2.97079
cTEL	970.0331	95.6324000	29.0207300	0.7547500	-0.31245500	3.09257	2.97762
cTEL	971.2831	96.8073000	29.1644100	0.7536760	-0.33067600	3.09453	2.98506
hCF49UR	995.9421	168.6030000	40.7849000	1.2281600	-0.58697500	3.12718	3.10608
hCF49UR	996.1897	172.8792000	40.0692000	1.2473000	-0.58240300	3.12739	3.10717
hCA01LD	1013.1350	159.1302000	59.5410000	1.4045900	-0.69785200	3.14025	3.17811
hCA01LD	1014.8114	151.2675000	64.1525000	1.3937700	-0.71906600	3.14184	3.18261
cTEL2	1036.4295	71.0990000	147.5033000	1.2541800	-0.99269000	3.17255	3.21882
cTEL2	1037.5834	67.9163200	153.2097000	1.2462000	-1.00795000	3.17495	3.22005
cTEL2	1038.8334	64.5962000	159.5319000	1.2375300	-1.02447000	3.17767	3.22132
hCA48LD	2014.3728	169.7869000	15.7209300	0.1156790	-0.09252040	6.36292	6.50436
IMB0	2074.4237	0.2949410	0.3168480	0.0106778	0.01719230	6.62890	6.84597
isPSYNC	3158.2980	52.7097000	114.6217000	1.6657200	-0.57609500	10.37325	10.35577
isPBSYNC	3170.8202	37.5764000	109.3306000	1.2479400	-0.60311700	10.41423	10.37556
IMD0	4168.8188	0.5070261	0.5086387	0.0136471	-0.00767506	13.76973	13.84953
hCD171LD	4383.8802	88.1358000	34.6483000	5.1377300	0.00652457	14.79817	14.72322
hCD171LD	4383.8802	88.1358000	34.6483000	5.1377300	0.00652457	14.79817	14.72322
hCD172UR	4389.6127	71.1773000	44.5317000	4.6538500	0.01683230	14.80885	14.74892
hCD172UR	4392.7256	63.0902000	51.1540000	4.3910800	0.02242980	14.81575	14.76012
hCD173LD	4392.9003	62.6599000	51.5517000	4.3763400	0.02274380	14.81616	14.76070
hCD173LD	4394.5767	58.6560000	55.5107000	4.2348300	0.02575820	14.82030	14.76602
hCD49UR	5184.2316	86.3920000	79.6735000	2.6897100	0.36098900	17.27173	17.24713
hCD49UR	5184.4792	84.3673000	81.9794000	2.6593500	0.36563500	17.27215	17.24767
hCE01UR	5197.1643	60.4420800	103.1548000	2.2804400	0.38480800	17.30169	17.26839
hCE01UR	5198.8407	61.3391100	100.2632000	2.2934600	0.37554200	17.30568	17.27122
hCE02LD	5235.5002	107.1816000	62.0208000	2.5782300	0.17290900	17.37728	17.34896
hCE02LD	5237.1766	110.4773000	61.4147000	2.5912500	0.16364300	17.37977	17.35303
hCE03UR	5237.3544	110.8331000	61.3564000	2.5926300	0.16266000	17.38003	17.35347
hCE03UR	5239.0308	114.2448000	60.8608000	2.6056500	0.15339400	17.38246	17.35755

Table 2: Tevatron lattice functions at collimators. Measurements of 20 Aug 2010.

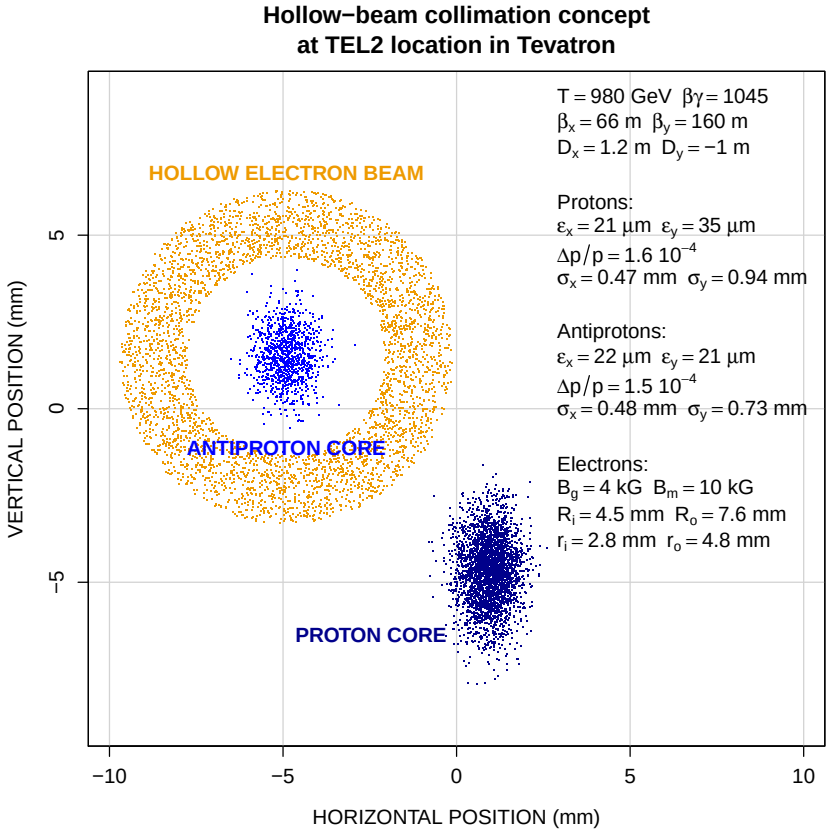

List of devices: intensities, sizes, tunes, tune and chromaticity settings, luminosities, losses, collimator positions, TEL2 settings.

7.2 Store 8171, 13–14 Oct 2010

Acting on A13 and A25. Horizontal pos., vertical pos. and horizontal angle scans. Pulsing patterns: skip 0 and skip 5. 3 hole sizes.

Comparison of skip 0 and skip 5 in horizontal scan.

Losses, intensity lifetimes, and luminosity lifetimes during scans.

Observables vs. hole size.

7.3 Store 8210, 27–28 Oct 2010

'Official' demonstration of parasitic operations. Effect of working point on losses. Intensity and luminosity decay rates vs. e-current over 10 min. Vertical orbit bump with fixed e-beam.

7.4 Store 8349, 9 Dec 2010

Size of hole with vertical orbit bump: single bunch vs. whole train, no difference. 4–7–4 kG, A18 and A13–A24. Vacuum instability at high currents.

7.5 Store 8365, 15 Dec 2010

Effects on lifetimes over medium term (30 min – 1 hr) on A18. Skip 5, 4–7–4 kG and 4–10–4 kG. Skip 0, 4–10–4 kG, demonstrated halo scraping with no effect on luminosity. Tried 2nd train, no effect?

7.6 Store 8415, 11 Jan 2011

Lens on A18 at 4 different current settings for at least 1 hr with 5σ hole. Measured intensity and luminosity lifetimes.

'Retracting' the collimator by decreasing the main solenoidal field.

Same as first experiments, 20 minutes for each current setting, 4σ hole.

7.7 Store 8430, 19 Jan 2011

Pulsing on antiproton train 2 (A13–A24) with 4.5σ hole with intensity up to T:L2MCV1=450 V (440 mA peak). Short study due to beam abort caused by C:D0Q3 power supply trip.

7.8 Store 8466, 31 Jan 2011

Pulsing on antiproton train 2 (A13–A24) with 4.5σ (45 min) and 5σ (1.5 h) hole with intensity up to T:L2MCV1=590 V (547 mA peak).

7.9 Store 8467, 3 Feb 2011

Dedicated studies at the end of a very long store. All collimators out except F49 pbar target. Pulsing on antiproton train 2 (A13–A24) with 3.5σ hole (1.29–2.19 mm at F49), 150 mA. Beam size at F49: $\sigma_y = 370\ \mu$m. Small vertical collimator steps (about 50 μm) in and out to see if we can measure the diffusion rate vs. amplitude. A loss monitor at E11 triggered a beam abort during one of the inward steps because we were also scraping protons (small vertical separation of the orbits).

7.10 Store 8508, 17 Feb 2011

Collimator scans in small steps with F48 vertical to measure halo population and diffusion rates: 1) normal conditions and 2) HEBC at 3.5 sigma on all 3 trains (140 mA). Recorded some frequency spectra of losses with lens on and off.

7.11 Store 8527, 25 Feb 2011

End of very long store. Collimator scans in small steps with F48 vertical to measure halo populations and diffusion rates: 1) normal conditions and 2) HEBC at 3.8 sigma on all 3 trains (100 mA). Set collimator close to elens, pulsing on only train 2 (400 mA): observed increase in local losses and no increase in losses at experiments (improvement in collimation efficiency?).

7.12 Store 8546, 3 Mar 2011

Parasitic experiments with hollow beam on 2nd antiproton train for 7 different values of the hole size: 6 sigma, 5.5, 5, 4.5, 4, 3.75, 3.5. Approximately same total current (400 mA) in each case. Good measurements of removal rates, effects on luminosity, emittances, and collimation efficiency vs. hole size. Reduction in fluctuations for a given loss level?

7.13 Store 8709, 4 May 2011

Pulsing on train 2 (A13-A24) and on half of train 2 (A13-A18). Different hole sizes and beam currents:

Hole size sigma_y	Bunches	T:L2MCV1 V	T:L2COLI mA	peak current mA
4.5	A13-A24	598	85.75	
4.0	A13-A24	564	86.98	453
3.75	A13-A24	526	86.98	
3.5	A13-A24	505	86.98	
3.5	A13-A24	599	99.5	
3.5	A13-A24	350	60	
3.5	A13-A24	265	40	
4.0	A13-A18	598	73	864
4.0	A13-A18	430	53	

Tested new loss monitors at the pbar collimators gated to each bunch train (T:LF49T1, T2, and T3). The response to losses induced by the e-lens is good: 1e4 to 1e5 counts on top of 5e4 for e-beam currents of 0.4-0.8 A and hole sizes between 3.5 and 4.5 sigma.

Acquired data on removal rates and collimation efficiencies at different hole sizes and beam currents. In general, we see that when the lens induces losses, the fraction captured by the collimators relative to C:D0AH increases significantly.

If we need to only see losses from a smaller number of bunches, the quickest thing to try is to slide the window trigger delay T:LA0DLY. This will pick up abort gap losses, but they should not be too large.

Preliminary measurements of collimation efficiency and loss spikes by train.

7.14 Store 8733, 13 May 2011

Collimator baby steps in and out at hole radius = 5 sigma, acting on pbar bunch train #2 with about 400 mA e-beam current. Collimator baby steps out at hole radius = 4 sigma, train #2, 400 mA. By comparing the antiproton loss monitors gated to each train, the effect of the electron lens on diffusion rates and steady-state losses is very clear, especially at 4 sigma moving out.

7.15 Store 8749, 20 May 2011

Collimator scans (F48 vertical) with hollow electron beam on bunches A19-A24 of Train #2 with 3 different peak currents: 872 mA (inward and outward), 611 mA, and 318 mA (a few steps inward, then outward). The scans covered about 1.2 mm (more than 4 sigmas). Gated pbar loss monitors allowed us to do simultaneous measurements with affected and control bunches; the window was shifted (from 217 rfc to 343 rfc) to cover only the second half of each train and part of the abort gap. Effect of the electron beam on diffusion times and fluctuations in losses is very clear. Probably good data also for intensity lifetimes vs. collimator position.

7.16 Store 8763, 24 May 2011

Scanned pulsing pattern: skip 0 (every turn), 1 (every other turn), 2 (every three turns), 3, 4, and 5 with elens on pbar bunches A19-A24. Measured intensity, luminosity, losses, emittance growth, Schottky spectra. It seems that every pattern except skip 0 makes luminosity decrease more than intensity. The effect is strongest for skip 5, where emittance growth is obvious. At skip 1, observed coherent lines in vertical Schottky spectrum. At skip 4, very strong coherent line at 0.6 (maybe related to protons). We decided not to go high in current. Collected good data for comparisons with simulations.

7.17 Store 8764 (pbar only), 24 May 2011

Pbar only store with bunches A1-A4 and A13-A16. Measured removal rates, losses, and emittances with elens on A13-16, skip 0, 832 mA peak, 4.5 sigma hole radius (4-13-4 kG). Measured diffusion rates vs. amplitude for affected and control trains with F48 vertical collimator steps. Scan was done twice to estimate effect of horizontal collimator (half way in the first time, out the second time). A couple of fast collimator scans (inward and outward) to estimate halo populations. With elens on, observed a shoulder similar to the crystal collimator scans; may be due to particle accumulation or enhanced diffusion or both. Preliminary conclusions: removal rate is the same as with colliding beams; diffusion of affected train is dominated by e-lens; diffusion of control train is much slower without beam-beam (about 1 order of magnitude).

7.18 Extinction scans at 150 GeV, 27 May 2011

Measured the extinction point of 150-GeV protons with collimators F48, F49, D17(2), and E0(3), both horizontally and vertically, to calibrate their positions relative to the BPMs.

7.19 Store 8816, 14 June 2011

Long-term study of the effects of the hollow beam collimator. Electron beam on pbar bunches A19–A24 for most of Store #8816, 816 mA peak, 4/12.7/4 kG configuration (5.75 sigma at beginning of store, inside collimators). Slow pbar orbit drift; e-beam position corrected (0.25 mm) around 00:30. Java TEL2 BPM program stopped reporting shortly after 00:30. Observed slow scraping of intensity (fraction of a %/h) with both misaligned beams (0.25 mm, about 1/2 sigma at TEL2) and with beam sigma above 0.4 mm at SyncLite. Note: intentional beam misalignment may be a faster and safer way to scrape at the beginning of a store, as opposed to shrinking the hole radius. No adverse effects on emittances. Effect on luminosity was almost negligible. Analysis of all 6 bunches is needed to make quantitative statements. Observed suppression of loss spikes during tune changes. Almost no effect on loss spikes due to beam jitter. This may be expected: collimators were at their usual loose settings (6 sigma or more), and the e-lens was just inside.

7.20 Store 8820, 16 June 2011

As in the previous study, the hollow electron beam was left on for most of the collider store, acting on pbar bunches A19–A24 plus a slot in the following abort gap (for monitoring e-beam position). Used smaller hole with constant physical radius (4/13.5/4 kG) and intentional misalignment (0.5 mm downward) at the beginning of the store. Starting measurements at the beginning of the store allows one to see the effects of tune changes. Collected data on removal rates, emittances, luminosities, loss rates.

7.21 To do

- Long-term scraping of 1 train over a whole collider store: probably parasitic
- E-lens on protons (if we can make them small enough by not coalescing, scraping, reducing intensities, ...): 6 h proton only or special collider store, dedicated
- Effects on halo with pixel detector, if possible (does it require acting on protons?): 3 h, dedicated
- E-beam position scans with gated loss monitors: 3 h, dedicated

7.22 Conclusions so far

7.22.1 Basics

- Effects are detectable.
- Other bunches, including proton outside, are not affected.
- When aligned, losses at experiments are small, can work parasitically.
- BPM alignment is reliable.

- Orbit bump with fixed e-beam is viable: bump is local and tunes are stable.
- Stable conditions for whole store duration.
- It is possible to work with a whole bunch train: stable conditions, same hole size.

7.22.2 Removal rates

- Particle removal is smooth and tunable.
- Removal is not dependent on beam-beam (verified with pbar only).

7.22.3 Enhancement of diffusion

- Diffusion is enhanced by factor 10 with 1 A.

7.22.4 Effects on core

- Different intensity/luminosity decay rate.
- No additional emittance growth, scraping of tails.
- Measured removal rate vs. amplitude with collimator scans.

7.22.5 Fluctuations in losses

- Loss spikes due to low-frequency beam jitter are suppressed.

7.22.6 Pulsing

- Pulsing is much more effective than every turn.
- Pulsed mode very sensitive to tunes and chromaticity.
- Pulsed mode causes coherent spikes in Schottky spectrum.
- In pulsed mode, luminosity is affected: field imperfections? bends?

7.22.7 Issues, not understood

- Current is limited when pulsing every turn on a whole bunch train: anode power supply?
- Vacuum instability at high currents (whole train) and low fields: secondary electrons? collector heating?
- Unexpected losses on protons outside during vertical orbit bump: change in coupling (h/v kicks)?

8 Proposed design for the LHC upgrade

8.1 Motivation and strategy

Scraping before collisions, scraping before collimator setup, reduce impedance, improve efficiency for ions, mitigate crab cavity failures (machine protection).

Conceptual design in 2013, detailed technical design in 2014, construction starting in 2015, installation in 2018 (LS2).

Synergies with electron cooler (BE-BI).

8.2 Physical parameters

Removal rates.

Effects on core.

Pulse time structure.

Lifetrac and Sixtrack results for Tevatron, SPS, and LHC.

Impedance. Can slow electrons induce coupled-bunch instabilities in LHC (transit time $\sim$30 ns, bunch spacing 25 ns)? In Tevatron, no instabilities with DC beam. Instability thresholds to be studied (vs B field, e current, e size, alignment, ...).

Candidate locations: RB-44 or RB-46 near IR4.

8.3 Engineering

Mechanical design. Vacuum. Cryogenics. Integration. Reuse TEL solenoids and spare support? Contact: Francesco Bertinelli (CERN EN-MME).

8.4 Instrumentation and controls

BE-BI ownership. Test stand. Modulator. Diagnostics. Controls. Need for beam halo diagnostics. Contact: Rhodri Jones (CERN BE-BI).

8.5 Preliminary tests at RHIC?

Not tested at Tevatron: protons, pulsed mode, dynamical use during ramp or squeeze. Unlikely because of RHIC run schedule.

8.6 Alternative schemes

Tune modulation.

Noise in transverse damper.

References

[1] Church et al., Tev collimators, 1999

[2] LHC Design Report

[3] Shiltsev, Valencia, CERN-2007-002

[4] Shiltsev et al., EPAC08

[5] Shiltsev et al., PRSTAB 2008

[6] Shiltsev et al., New J. Phys. **10**, 043042 (2008)

[7] Zhang et al., PRSTAB **11**, 051002 (2008)

[8] Burov, PRE

[9] Smith et al., PAC09